CLM - P 498

UKAEA RESEARCH GROUP

Preprint

ELLIPTIC EQUATIONS IN FUSION RESEARCH AND RELATED FIELDS

C. LI. THOMAS

CULHAM LABORATORY
Abingdon Oxfordshire

1977

CLM-P498

ELLIPTIC EQUATIONS IN FUSION RESEARCH AND RELATED FIELDS

C.Ll. Thomas

Culham Laboratory, Abingdon, Oxon, OX14 3DB, UK
(Euratom/UKAEA Fusion Association)

(To appear in Computers, Fast Elliptic Solvers and Applications - Proceedings of the G.A.M.M. Workshop on Fast Solution Methods for the Discretized Poisson Equation, KFZ Karlsruhe, Federal Republic of Germany, 3-4 March 1977)

Abstract

We identify some areas of fusion research and related fields in which elliptic equations arise. The approach to solving potential problems in two dimensions is described in detail and the extensions to three dimensions and nonlinear equations are given. The use of both iterative and fast direct methods to solve these equations is described and the relative merits of the two approaches outlined.

July, 1977

ELLIPTIC EQUATIONS IN FUSION RESEARCH AND RELATED FIELDS

C. Ll. Thomas

Culham Laboratory, Abingdon, Oxon. OX14 3DB, UK
(Euratom/UKAEA Fusion Association)

1. INTRODUCTION

A self-sustaining thermonuclear reaction requires a plasma (a fully ionized, electrically conducting, neutral gas) to be held in a state of high temperature and high particle density for a sufficiently long time. At this high temperature direct contact between the plasma and any material container would cause serious contamination. A current line of research is to confine the plasma away from the container walls by applying a magnetic field. The design of such a field for advanced experiments frequently requires the solution of an elliptic equation if simplifying assumptions are made. In many of the present experiments a copper shell is used to enhance the stability of the plasma. The finite conductivity of the copper allows the magnetic field to diffuse through the shell. Although this is a time dependent problem, the fully implicit finite difference method is always used and as will be shown, requires an elliptic equation to be solved at every timestep. For an applied magnetic field it is important to know where the plasma will position itself in equilibrium. For a theoretical study it is usual to treat the steady state MHD* equations and under certain assumptions these reduce to a single nonlinear elliptic equation. Expertise in solving electrostatic problems has also been used at Culham Laboratory in applications outside the fusion field.

In this paper we describe the approach made to these problems at Culham Laboratory. In Section 2 we derive the differential equations for certain two dimensional electric and magnetic fields and outline the engineering and computational aspects of typical problems. In Section 3 we show how our approach was extended to treat three dimensional electric fields. We derive the differential equations for two dimensional magnetic flux diffusion in Section 4 and

*The MHD (magnetohydrodynamic) equations are a combination of Maxwell's equations and the fluid dynamic equations

describe the computational aspects of various problems. The two dimensional MHD equilibrium equation is derived in Section 5 and we show how the physics of the problem determines the computational approach. Finally in Section 6, we give two typical examples of solutions of elliptic equations in fusion research.

2. TWO DIMENSIONAL ELECTROSTATIC AND MAGNETIC FIELDS

An electrostatic field is produced when a potential difference is applied between two or more conductors or when the region between conductors is occupied by electrostatic charge. In the former situation, the region between the conductors may contain one or more insulators. Combining the two situations, the general problem is to solve

$$\underline{\nabla} \cdot \underline{D} = \rho \tag{1}$$

where φ is the electrostatic potential with $\underline{E} = -\underline{\nabla}\varphi$ and $\underline{D} = \epsilon \underline{E}$, $\underline{E}$ being the electrostatic field, $\underline{D}$ the electric flux density, ϵ the local absolute permittivity and ρ the local charge density. If the conductors form a closed region, we have sufficient boundary conditions to solve (1) since φ = constant on each conductor. If the region is not closed we must consider the behaviour at infinity and represent this by the appropriate boundary condition, frequently $\frac{\partial\varphi}{\partial n} = 0$ (uniform field). Symmetry about some line also gives this boundary condition.

The most frequently occurring two dimensional electric field is the cylindrically symmetric field. Introducing cylindrical coordinates (r, θ, z) and setting all derivatives $\frac{\partial}{\partial\theta} = 0$, (1) reduces to

$$\frac{1}{r}\frac{\partial}{\partial r}\left(\epsilon r \frac{\partial\varphi}{\partial r}\right) + \frac{\partial}{\partial z}\left(\epsilon \frac{\partial\varphi}{\partial z}\right) = -\rho \quad \text{when} \quad r \neq 0 \tag{2}$$

and

$$2\frac{\partial}{\partial r}\left(\epsilon \frac{\partial\varphi}{\partial r}\right) + \frac{\partial}{\partial z}\left(\epsilon \frac{\partial\varphi}{\partial z}\right) = -\rho \quad \text{when} \quad r = 0 \tag{3}$$

In rectangular cartesian coordinates (x, y, z) a field can be considered to be two dimensional if effects in two coordinate directions are much more pronounced than in the third direction. Assuming that this third direction is the z direction, (1) reduces to

$$\frac{\partial}{\partial x}\left(\epsilon\frac{\partial\varphi}{\partial x}\right) + \frac{\partial}{\partial y}\left(\epsilon\frac{\partial\varphi}{\partial y}\right) = -\rho \tag{4}$$

Magnetic fields are produced by currents flowing in conductors. Frequently iron occupies part of the region between the conductors. If the currents are D.C., we know the current density in the conductors but the region between the conductors is typically infinite. In the A.C. case and in the limit of high frequency or high conductivity, the magnetic field becomes tangential to the surface of the conductor. The region between the conductors is usually closed. Hence we have two special cases of the general problem

$$\begin{aligned} \underline{\nabla} \times \underline{H} &= \underline{j} \\ \underline{\nabla} \cdot \underline{B} &= 0 \end{aligned} \tag{5}$$

where $\underline{A}$ is the magnetic vector potential with $\underline{B} = \mu\underline{H}$ and $\underline{B} = \underline{\nabla} \times \underline{A}$. $\underline{B}$ is the magnetic flux density, $\underline{H}$ is the magnetic field, μ is the local absolute permeability, and $\underline{j}$ is the local current density.

The most common two dimensional magnetic fields in fusion research are axisymmetric. Using cylindrical coordinates (r, φ, z) and setting all derivatives $\frac{\partial}{\partial\varphi} = 0$, we can introduce a stream function ψ, where $B_r = -\frac{1}{r}\frac{\partial\psi}{\partial z}$ and $B_z = \frac{1}{r}\frac{\partial\psi}{\partial r}$. Since currents only flow in the φ direction it is easy to show that ψ satisfies the equation

$$r\frac{\partial}{\partial r}\left(\frac{1}{\mu r}\frac{\partial\psi}{\partial r}\right) + \frac{\partial}{\partial z}\left(\frac{1}{\mu}\frac{\partial\psi}{\partial z}\right) = -rj_\varphi \tag{6}$$

and rB_φ = constant. Now $\underline{B} \cdot \underline{\nabla}\psi = 0$, so the magnetic field lines are the contours of ψ. In rectangular cartesians (x, y, z) with negligible effects in the z direction, we introduce a stream function ψ where $B_x = \frac{\partial\psi}{\partial y}$ and $B_y = -\frac{\partial\psi}{\partial x}$. Since currents flow only in the z direction, it is easy to show that ψ satisfies

$$\frac{\partial}{\partial x}\left(\frac{1}{\mu}\frac{\partial\psi}{\partial x}\right) + \frac{\partial}{\partial y}\left(\frac{1}{\mu}\frac{\partial\psi}{\partial y}\right) = -j_z \tag{7}$$

and B_z = constant. Once again $\underline{B}.\underline{\nabla}\psi = 0$. Hence both these two dimensional fields are the solution of a scalar equation, whereas the full three dimensional field requires the solution of a coupled set of three vector equations.

In D.C. fields the longitudinal current density is known and the artificial boundary conditions are $\psi \to 0$ at $r = 0$ and $r = \infty$ in the axisymmetric case for example. In A.C. fields, the current density is

zero, but we know that ψ = constant on each conductor. The constants cannot normally be specified a priori but comparison of $\int \underline{H} \cdot d\underline{\ell} = I$ around each conductor with the known value of the current allows a certain amount of scaling of the constants.

In general, therefore, the computation of a two dimensional electric or magnetic field requires the solution of a self-adjoint variable coefficient linear elliptic equation

$$a(x_1,x_2)\frac{\partial}{\partial x_1}\left(b(x_1,x_2)\frac{\partial\varphi}{\partial x_1}\right) + \frac{\partial}{\partial x_2}\left(c(x_1,x_2)\frac{\partial\varphi}{\partial x_2}\right) = g(x_1,x_2) \qquad (8)$$

inside a general two dimensional region on whose boundary either φ or $\frac{\partial\varphi}{\partial n}$ is specified.

The finite difference method has proved adequate for most problems encountered at Culham. Most geometries are complicated so a variable spacing rectangular grid is used. The user image of the code POTENT is described elsewhere, /133/. Here we will give a resumé of the numerical techniques.

Using Gauss' Law, equation (1) can be written as

$$\int_S \epsilon\frac{\partial\varphi}{\partial n}\, dS = -\int_V \rho dV \qquad (9)$$

where S is a 3 dimensional closed surface with volume V and unit outward normal $\underline{n}$. This formulation leads to a natural treatment of the Neumann boundary condition $\frac{\partial\varphi}{\partial n} = f$. In two dimensions we replace the surface integral by a line integral and the volume integral by a surface integral. Consider the point P in Figure 1. The curve S is made up of the perpendicular bisectors of the grid lines joining P to its 4 neighbours. The difference equation at P is constructed by approximating (9) on this cell. The grid lines divide this rectangle into 4 parts and we assume that ϵ is constant in each of these. This effectively replaces any sloping interface by a step interface coinciding with the grid lines. More sophisticated representations of the interface have not produced any significant improvement in accuracy. It would appear that finite differences on a rectangular grid are not well suited to sloping interfaces and an accurate treatment is only possible with a finite element approach. With this approximation we evaluate $\int_S \epsilon d\ell$ exactly and replace $\frac{\partial\varphi}{\partial n}$ by a central difference, taking it as constant along each side. The resulting

difference equation is

$$\frac{\varphi_N - \varphi_P}{H_N}\frac{1}{2}(H_E\,\epsilon_{NE} + H_W\,\epsilon_{NW}) + \frac{\varphi_S - \varphi_P}{H_S}\frac{1}{2}(H_E\,\epsilon_{SE} + H_W\,\epsilon_{SW})$$

$$+\frac{\varphi_E - \varphi_P}{H_E}\frac{1}{2}(H_N\,\epsilon_{NE} + H_S\,\epsilon_{SE}) + \frac{\varphi_W - \varphi_P}{H_W}\frac{1}{2}(H_N\,\epsilon_{NW} + H_S\,\epsilon_{SW})$$

$$= -\rho_p\frac{1}{4}(H_N + H_S)(H_E + H_W) \tag{10}$$

where $\epsilon_{NE} = \epsilon(x_p + \frac{1}{2}H_E,\ y_p + \frac{1}{2}H_N)$ etc.

In cylindrical coordinates, the procedure is along the same lines but we evaluate (9) on the shape in Fig.2 when $r_p \neq 0$ and on the shape in Fig. 3 when $r_p = 0$. The resulting difference equations are

$$\frac{\varphi_N - \varphi_P}{H_N}(r_p + \frac{1}{2}H_N)\frac{1}{2}(H_E\,\epsilon_{NE} + H_W\,\epsilon_{NW}) + \frac{\varphi_S - \varphi_P}{H_S}(r_p - \frac{1}{2}H_S)\frac{1}{2}(H_E\,\epsilon_{SE} + H_W\,\epsilon_{SW})$$

$$+\frac{\varphi_E - \varphi_P}{H_E}\frac{1}{2}\{[(r_p + \frac{1}{2}H_N)^2 - r_p^2]\epsilon_{NE} + [r_p^2 - (r_p - \frac{1}{2}H_S)^2]\epsilon_{SE}\}$$

$$+\frac{\varphi_W - \varphi_P}{H_W}\frac{1}{2}\{[(r_p + \frac{1}{2}H_N)^2 - r_p^2]\epsilon_{NW} + [r_p^2 - (r_p - \frac{1}{2}H_S)^2]\epsilon_{SW}\}$$

$$= -\rho_p\frac{1}{4}[(r_p + \frac{1}{2}H_N)^2 - (r_p - \frac{1}{2}H_S)^2](H_E + H_W) \tag{11}$$

when $r_p \neq 0$ and

$$\frac{\varphi_N - \varphi_P}{H_N}\frac{1}{2}H_N\frac{1}{2}(H_E\,\epsilon_{NE} + H_W\,\epsilon_{NW}) + \frac{\varphi_E - \varphi_P}{H_E}\frac{1}{2}(\frac{1}{2}H_N)^2\,\epsilon_{NE}$$

$$+\frac{\varphi_W - \varphi_P}{H_W}\frac{1}{2}(\frac{1}{2}H_N)^2\,\epsilon_{NW} = -\rho_p\frac{1}{2}(H_E + H_W)\frac{1}{2}(\frac{1}{2}H_N)^2 \tag{12}$$

when $r_p = 0$.

A similar treatment is available for magnetic problems if we consider Ampere's Law

$$\int_C \frac{1}{\mu}\,\underline{\nabla}\times\underline{A}\cdot d\underline{\ell} = \int_S \underline{j}\cdot\underline{n}\,dS \tag{13}$$

where S is a 2 dimensional surface with unit outward normal $\underline{n}$, bounded by a curve C with tangent vector $\underline{\ell}$.

In rectangular cartesians (13) can be reduced to

$$\int_c \frac{1}{\mu} \frac{\partial\psi}{\partial n} \, d\ell = - \int_s j_z \, dS \tag{14}$$

and approximation of (14) on the shape in Fig.1 gives the difference equation

$$\frac{\psi_N - \psi_P}{H_N} \frac{1}{2} \left(\frac{H_E}{\mu_{NE}} + \frac{H_W}{\mu_{NW}} \right) + \frac{\psi_S - \psi_P}{H_S} \frac{1}{2} \left(\frac{H_E}{\mu_{SE}} + \frac{H_W}{\mu_{SW}} \right)$$

$$+ \frac{\psi_E - \psi_P}{H_E} \frac{1}{2} \left(\frac{H_N}{\mu_{NE}} + \frac{H_S}{\mu_{SE}} \right) + \frac{\psi_W - \psi_P}{H_W} \frac{1}{2} \left(\frac{H_N}{\mu_{NW}} + \frac{H_S}{\mu_{SW}} \right)$$

$$= - j_{zp} \frac{1}{4} (H_N + H_S)(H_E + H_W) \tag{15}$$

In cylindrical coordinates (13) can be reduced to

$$\int_c \frac{1}{\mu r} \frac{\partial\psi}{\partial n} d\ell = - \int_s j_\varphi \, dS \tag{16}$$

If we identify the r and z directions with the x and y directions, respectively in Fig.1, the difference equation for (16) becomes

$$\frac{\psi_N - \psi_P}{H_N} \frac{1}{r_p} \frac{1}{2} \left(\frac{H_E}{\mu_{NE}} + \frac{H_W}{\mu_{NW}} \right) + \frac{\psi_S - \psi_P}{H_S} \frac{1}{r_p} \frac{1}{2} \left(\frac{H_E}{\mu_{SE}} + \frac{H_W}{\mu_{SW}} \right)$$

$$+ \frac{\psi_E - \psi_P}{H_E} \frac{1}{\left(r_p + \frac{1}{2} H_E\right)} \frac{1}{2} \left(\frac{H_N}{\mu_{NE}} + \frac{H_S}{\mu_{SE}} \right) + \frac{\psi_W - \psi_P}{H_W} \frac{1}{\left(r_p - \frac{1}{2} H_W\right)} \frac{1}{2} \left(\frac{H_N}{\mu_{NW}} + \frac{H_S}{\mu_{SW}} \right)$$

$$= - j_{\varphi p} \frac{1}{4} (H_N + H_S) (H_E + H_W) \tag{17}$$

$r_p = 0$ does not concern us since magnetic field lines cannot cross the axis of a cylindrical system. Hence the line $r_p = 0$ is always a boundary of the problem.

When the point P has one or more neighbours outside the region of the problem, we must modify the difference equation by using the boundary conditions to eliminate the exterior point(s). The modifications and the procedure for automatically setting up the difference equations are described in /133/.

A comparison of (10), (11), (12), (15) and (17) shows that provided we have some Dirichlet boundary conditions, the matrix of difference coefficients is strictly diagonally dominant with 5 entries per row, the off-diagonal elements non-negative and the diagonal elements negative. The arbitrary shape of the boundary, the variable mesh in each direction and the material properties varying in both directions together all preclude the use of a fast Poisson solver. However iterative methods are well known to be convergent for these matrices but are of course appreciably slower than fast Poisson solvers. Since the equations only have to be solved once in any run, this is no great disadvantage. The code allows the equation to be solved by one of three iterative methods - ADI, SOR or SLOR. Experience with many problems shows that SLOR is always satisfactory, see /133/.

With the flexibility of a variable mesh we must provide guidelines for placing the grid if efficient use is to be made of the code. It is not always possible to keep to these guidelines strictly as the number of mesh points in each direction is restricted by computer storage. When adjacent mesh spacings are of different lengths, the local truncation error is proportional to the difference between the two spacings. This source of error is reduced if adjacent mesh spacings vary smoothly. Little /*1/ has arrived at the empirical rules that the ratio between adjacent mesh spacings in the same direction should never be greater than 2 : 1 and the ratio between the maximum grid spacing in one direction and the minimum grid spacing in the other should not be greater than 10 : 1. This gives satisfactory convergence and accuracy, see Section 6.

The finite difference method has the drawback that it can only treat interior problems. Hence exterior problems must be turned into interior problems by introducing artificial boundaries at infinity. The smaller the area of the artificial boundary, the fewer the number of grid points which must be placed in the physically uninteresting parts of the exterior region. Little has demonstrated that the radius of the artificial boundary need only be 6 times the maximum radius of the physical boundaries, for acceptable accuracy.

3. THREE DIMENSIONAL ELECTROSTATIC FIELDS

As experiments and equipment have become more sophisticated the need to go to three dimensions has arisen. Electrostatic fields remain scalar in three dimensions and the rectangular cartesian equation is

$$\frac{\partial}{\partial x}\left(\epsilon \frac{\partial \varphi}{\partial x}\right) + \frac{\partial}{\partial y}\left(\epsilon \frac{\partial \varphi}{\partial y}\right) + \frac{\partial}{\partial z}\left(\epsilon \frac{\partial \varphi}{\partial z}\right) = - \rho \tag{18}$$

The code THREED /134/ is a completely logical extension of POTENT and the two user images have been kept as close as possible. The procedure for deriving the difference equations follows the lines of the two dimensional procedure. Gauss' Law, equation (9) is approximated on the mesh cell shown in Fig.4 where each side of the cell is the perpendicular bisecting plane of the grid line joining P to the appropriate neighbour. ϵ is taken as constant in each 'eighth' of the cell, $\frac{\partial \varphi}{\partial n}$ is taken as constant over each side of the cell and $\int \epsilon dS$ is evaluated exactly. The resulting difference equation is

$$\begin{aligned}
&\frac{\varphi_E - \varphi_P}{H_E} \frac{1}{4} (H_S H_B \epsilon_{SBE} + H_N H_B \epsilon_{NBE} + H_N H_T \epsilon_{NTE} + H_S H_T \epsilon_{STE}) \\
&+ \frac{\varphi_W - \varphi_P}{H_W} \frac{1}{4} (H_S H_B \epsilon_{SBW} + H_N H_B \epsilon_{NBW} + H_N H_T \epsilon_{NTW} + H_S H_T \epsilon_{STW}) \\
&+ \frac{\varphi_N - \varphi_P}{H_N} \frac{1}{4} (H_W H_B \epsilon_{NBW} + H_E H_B \epsilon_{NBE} + H_E H_T \epsilon_{NTE} + H_W H_T \epsilon_{NTW}) \\
&+ \frac{\varphi_S - \varphi_P}{H_S} \frac{1}{4} (H_W H_B \epsilon_{SBW} + H_E H_B \epsilon_{SBE} + H_E H_T \epsilon_{STE} + H_W H_T \epsilon_{STW}) \\
&+ \frac{\varphi_T - \varphi_P}{H_T} \frac{1}{4} (H_S H_W \epsilon_{STW} + H_N H_W \epsilon_{NTW} + H_N H_E \epsilon_{NTE} + H_S H_E \epsilon_{STE}) \\
&+ \frac{\varphi_B - \varphi_P}{H_B} \frac{1}{4} (H_S H_W \epsilon_{SBW} + H_N H_W \epsilon_{NBW} + H_N H_E \epsilon_{NBE} + H_S H_E \epsilon_{SBE}) \\
&= - \rho_p \frac{1}{8} (H_E + H_W)(H_N + H_S)(H_T + H_B)
\end{aligned} \tag{19}$$

where

$$\epsilon_{SBW} = \epsilon(x_p - \tfrac{1}{2} H_W,\ y_p - \tfrac{1}{2} H_S,\ z_p - \tfrac{1}{2} H_B) \text{ etc}$$

Boundary conditions are incorporated in a way analogous to the two dimensional approach. The matrix of difference equations has all the

properties of the matrix occuring in the two dimensional problem, but has 7 entries per row instead of 5. Once again a fast Poisson solver is not applicable, but SOR and SLOR give acceptable convergence. We have not considered ADI since it is well known that in three dimensions optimum parameters are not available even in the simplest case, see /140/.

4. TWO DIMENSIONAL MAGNETIC FLUX DIFFUSION

A time varying magnetic field will induce an electric field in a conductor. Because of the finite conductivity of the material, the electric field sets up a current which in turn has a magnetic field. The net result of these magnetic fields is diffusion of the magnetic field into the conductor. Formally, we combine

Ohm's Law $\quad \underline{j} = \sigma \underline{E}$

and

Ampere's Law $\quad \underline{\nabla} \times \underline{H} = \underline{j}$

with the relationships $\quad \underline{E} = - \frac{\partial \underline{A}}{\partial t}$ (displacement currents can be neglected)

and $\quad \mu \underline{H} = \underline{\nabla} \times \underline{A}$

to give

$$\underline{\nabla} \times \frac{1}{\mu} \underline{\nabla} \times \underline{A} = - \sigma \frac{\partial A}{\partial t} \tag{20}$$

In rectangular cartesians (x, y, z) with $\frac{\partial}{\partial z} \equiv 0$ and $\psi = A_z$ we have

$$\frac{\partial}{\partial x}\left(\frac{1}{\mu}\frac{\partial \psi}{\partial x}\right) + \frac{\partial}{\partial y}\left(\frac{1}{\mu}\frac{\partial \psi}{\partial y}\right) = \sigma \frac{\partial \psi}{\partial t} \tag{21}$$

and in cylindrical polars (r, θ, z) with $\frac{\partial}{\partial \theta} \equiv 0$ and $\psi = rA_\theta$ we have

$$r \frac{\partial}{\partial r}\left(\frac{1}{\mu r}\frac{\partial \psi}{\partial r}\right) + \frac{\partial}{\partial z}\left(\frac{1}{\mu}\frac{\partial \psi}{\partial z}\right) = \sigma \frac{\partial \psi}{\partial t} \tag{22}$$

σ is the conductivity of the material and of course is zero outside a conductor. Hence we have an elliptic equation to solve outside the conductor and a parabolic equation to solve inside the conductor.

The standard approach is to use the fully implicit finite difference method, see Richtmyer and Morton /*2/. Hence at a point inside a conductor, the local equation is (assuming constant μ)

$$\frac{\psi_N^{n+1} - \psi_P^{n+1}}{H_N} \frac{1}{2}(H_E + H_W) + \frac{\psi_S^{n+1} - \psi_P^{n+1}}{H_S} \frac{1}{2}(H_E + H_W) + \frac{\psi_E^{n+1} - \psi_P^{n+1}}{H_E} \frac{1}{2}(H_N + H_S)$$

$$+ \frac{\psi_W^{n+1} - \psi_P^{n+1}}{H_W} \frac{1}{2}(H_N + H_S) = \sigma_p \mu_p \frac{\psi_P^{n+1} - \psi_P^{n}}{\Delta t} \frac{1}{4}(H_N + H_S)(H_E + H_W) \tag{23}$$

and at a point outside a conductor, the local equation is

$$\frac{\psi_N^{n+1} - \psi_P^{n+1}}{H_N} \frac{1}{2}(H_E + H_W) + \frac{\psi_S^{n+1} - \psi_P^{n+1}}{H_S} \frac{1}{2}(H_E + H_W) + \frac{\psi_E^{n+1} - \psi_P^{n+1}}{H_E} \frac{1}{2}(H_N + H_S)$$

$$+ \frac{\psi_W^{n+1} - \psi_P^{n+1}}{H_W} \frac{1}{2}(H_N + H_S) = 0 \tag{24}$$

Although the fully implicit method is recognized as cumbersome it has two main advantages for the flux diffusion problem. Firstly it can be shown that positivity is preserved by the difference equations. In other words, numerically computed fluxes are positive when the physical fluxes are positive - this is not always true with other difference schemes. Secondly we have a uniform treatment of all points in the grid.

Equation (23) can be manipulated so that all terms on the left-hand side are at the advanced time. We now have a set of equations to solve at each time step. The similarity between this set of equations and the equations for a static magnetic field is immediately apparent, so we can use all our techniques for setting up equations and for solving them. To complete the statement of the problem we need initial conditions and boundary conditions. Typically the boundary conditions are at infinity but in some situations it is necessary to impose the flux variation on a conductor (sinusoidal or an initial rise which is crowbarred). Imposed flux variations are analogous to source terms in (20).

Most present experiments are toroidal and a rectangular grid is not very suitable when the thickness of the copper shell is small compared with its minor radius. A toroidal polar (r,θ) grid is ideal for this problem especially when the shell has a circular cross-section. The difference equations are derived from Ampere's law

$$\int_c \frac{1}{R}\frac{\partial\psi}{\partial n}\, d\ell = \int_s \frac{\sigma\mu}{R}\frac{\partial\psi}{\partial t}\, dS \qquad (25)$$

where $R = R_o + r\cos\theta$, R_o being the distance from the axis of symmetry to the centre of the cross section of the shell. Evaluating (25) around the contour in Fig.5 in the usual manner we have:

$$\frac{\psi_N - \psi_P}{H_N}\left(r_p + \frac{1}{2}H_N\right)\frac{\delta\theta}{2}\left[\frac{1}{R_o + (r_p + \frac{1}{2}H_N)\cos(\theta_p - \frac{1}{2}\delta\theta)} + \frac{1}{R_o + (r_p + \frac{1}{2}H_N)\cos(\theta_p + \frac{1}{2}\delta\theta)}\right]$$

$$+ \frac{\psi_S - \psi_P}{H_S}\left(r_p - \frac{1}{2}H_S\right)\frac{\delta\theta}{2}\left[\frac{1}{R_o + (r_p - \frac{1}{2}H_S)\cos(\theta_p - \frac{1}{2}\delta\theta)} + \frac{1}{R_o + (r_p - \frac{1}{2}H_S)\cos(\theta_p + \frac{1}{2}\delta\theta)}\right]$$

$$+ \frac{\psi_E - \psi_P}{r_p\,\delta\theta}\frac{1}{2}(H_N + H_S)\frac{1}{2}\left[\frac{1}{R_o + (r_p + \frac{1}{2}H_N)\cos(\theta_p + \frac{1}{2}\delta\theta)} + \frac{1}{R_o + (r_p - \frac{1}{2}H_S)\cos(\theta_p + \frac{1}{2}\delta\theta)}\right]$$

$$+ \frac{\psi_W - \psi_P}{r_p\,\delta\theta}\frac{1}{2}(H_N + H_S)\frac{1}{2}\left[\frac{1}{R_o + (r_p + \frac{1}{2}H_N)\cos(\theta_p - \frac{1}{2}\delta\theta)} + \frac{1}{R_o + (r_p - \frac{1}{2}H_S)\cos(\theta_p - \frac{1}{2}\delta\theta)}\right]$$

$$= \frac{\sigma_p\,\mu_p}{R_o + r_p\cos\theta_p}\frac{\partial\psi}{\partial t}_p\frac{1}{2}\,\delta\theta\,\left[(r_p + \frac{1}{2}H_N)^2 - (r_p - \frac{1}{2}H_S)^2\right] \qquad (26)$$

When $r_p = 0$ a special treatment is required. Equation (25) is now approximated around the contour in Fig.6. We have

$$\frac{\psi_{Ni} - \psi_P}{H_N}\frac{1}{2}H_N\delta\theta\,\frac{1}{2}\left[\frac{1}{R_o + \frac{1}{2}H_N\cos(\theta_{Ni} - \frac{1}{2}\delta\theta)} + \frac{1}{R_o + \frac{1}{2}H_N\cos(\theta_{Ni} + \frac{1}{2}\delta\theta)}\right]$$

$$+ \frac{\partial\psi}{\partial\theta}E\,\frac{1}{2}H_N\frac{1}{2}\left[\frac{1}{R_o + \frac{1}{2}H_N\cos(\theta_{Ni} + \frac{1}{2}\delta\theta)} + \frac{1}{R_o}\right]$$

$$+ \frac{\partial\psi}{\partial\theta}W\,\frac{1}{2}H_N\,\frac{1}{2}\left[\frac{1}{R_o + \frac{1}{2}H_N\cos(\theta_{Ni} + \frac{1}{2}\delta\theta)} + \frac{1}{R_o}\right]$$

$$= \frac{\sigma_p\mu_p}{R_o}\frac{\partial\psi}{\partial t}_p\frac{1}{2}\frac{1}{4}H_N^2\,\delta\theta \qquad (27)$$

Summing all contributions from $\theta = 0$ for $\theta = 2\pi - \delta\theta$, the terms involving $\frac{\partial\psi}{\partial\theta}$ all cancel and we have

$$\frac{1}{Q}\sum_{i=1}^{Q}\frac{\psi_{Ni}-\psi_P}{H_N}\,\frac{1}{2}\,H_N\,\delta\theta\,\frac{1}{2}\left[\frac{1}{R_o+\frac{1}{2}H_N\cos(\theta_{Ni}-\frac{1}{2}\delta\theta)}+\frac{1}{R_o+\frac{1}{2}H_N\cos(\theta_{Ni}+\frac{1}{2}\delta\theta)}\right]$$

$$=\frac{\sigma_p\mu_p}{R_o}\,\frac{\partial\psi}{\partial t^p}\,\frac{1}{8}\,H_N^2\,\delta\theta \qquad (28)$$

where Q is the number of angular divisions and the suffix Ni refers to the ith point on the radius $r = H_N$.

Equations (27) and (28) are now amenable to a treatment similar to that used previously in this paper.

5. TWO DIMENSIONAL MHD EQUILIBRIA

The computation of two dimensional MHD equilibria is an important aspect of fusion research for at least two reasons. Firstly we can determine the plasma position and current distribution and various equilibrium quantities which measure the efficiency of the confinement and indicate the local stability. Secondly the equilibrium provides the basis for MHD stability studies.

Assuming that the plasma is stationary in equilibrium, the force balance equation is satisfied i.e.

$$\underline{\nabla} p = \underline{j} \times \underline{B} \qquad (29)$$

where $\underline{j}$ and $\underline{B}$ have their usual meanings and p is the plasma pressure. In addition we have the two Maxwell equations

$$\underline{\nabla} \times \underline{H} = \underline{j} \qquad (30)$$

$$\underline{\nabla} \cdot \underline{B} = 0 \qquad (31)$$

If the system is axisymmetric we can introduce the stream function ψ, as in Section 2. Straightforward manipulation of (29) and (30) shows that ψ satisfies

$$r\frac{\partial}{\partial r}\,\frac{1}{r}\,\frac{\partial\psi}{\partial r}+\frac{\partial^2\psi}{\partial z^2}+FF'+r^2p'=0 \qquad (32)$$

where $F(= rB_\varphi)$ and p, the pressure are both arbitrary functions of ψ.

If the system is two dimensional in rectangular cartesians we introduce ψ and find that it satisfies

$$\frac{\partial^2\psi}{\partial x^2}+\frac{\partial^2\psi}{\partial y^2}+FF'+p'=0 \qquad (33)$$

where $F(= B_z)$ and p, the pressure are both arbitrary functions of ψ.

In practice the functions F and p are not arbitrary but are determined by underlying physical processes. The efficient modelling of these processes has still to be devised as there are several fundamental difficulties. Hence the standard practice is to choose functions which are thought to be 'reasonable'. The choice of boundary condition is more straightforward. For example, if the plasma is surrounded by a perfectly conducting wall, we can set $\psi = \text{constant}$ on the wall.

We can identify 4 classes of problem and each requires a different computational approach. We first consider the situation of the plasma boundary coinciding with a perfectly conducting wall, on which the longitudinal current density is non-zero. We note that in (32) $rj_\varphi = FF' + r^2p'$ and in (33) $j_z = FF' + p'$. Hence at the wall, we have $F(\psi_W)F'(\psi_W) + r^2p'(\psi_W) \neq 0$ in (32) for example, where $\psi = \psi_W$ on the boundary and we cannot have the trivial solution $\psi = \psi_W$. The number of non-trivial solutions for given functions F and p is an unsolved area of pure mathematics. For functions F and p which lead to a linear equation, however, we do know that the solution is unique if $\frac{\partial}{\partial\psi}(FF' + r^2p') \leq 0$.

The most powerful numerical method which can be used on (32) or (33) when F and p are reasonable analytic functions is Newton's method. Symbolically we write our set of difference equations as

$$A\underline{\psi} = G(\underline{\psi}) \tag{34}$$

where the coefficients of A are derived in the usual manner. Then Newton's method is

$$(A - \underline{G}'(\underline{\psi}^n))(\underline{\psi}^{n+1} - \underline{\psi}^n) = \underline{G}(\psi^n) - A\underline{\psi}^n \tag{35}$$

Since $G(\psi)$ does not involve any derivatives of ψ, the matrix on the left hand side of (35) is A with just its diagonal elements altered. Hence, provided $A - G'(\psi^n)$ is positive definite, we may use an iterative method to solve equation (35). In fact instead of completely inverting the matrix we only need to perform a few iterations per Newton step. If $A - G'(\psi^n)$ is not positive definite, iterative methods are not applicable. Nevertheless we are still able to solve a wider class of problems than if we were to use Picard's method, which is the standard use of Poisson solvers.

The second class of problems also have the plasma boundary coinciding with a perfectly conducting wall, but the longitudinal current density vanishes at the wall. Hence $\psi = \psi_W$ is a trivial solution to the differential equation.

There may well be physically interesting (non-trivial) solutions to the equation, but they will be eigenfunctions corresponding to particular parameter values. As an example we consider

$$L\psi + \lambda\, G(\psi) = 0 \qquad (36)$$

where L is either of the differential operators occurring in (32) and (33), and $\lambda G(\psi)$ is the appropriate source term. $\psi = 0$ on the boundary and $G(0) = 0$. The method of solution was developed by Feneberg and Lackner /*3/ and is similar to inverse iteration. The idea is based on the fact that a non-trivial solution of (36) will have a non-zero total current ie $I = \int \lambda H(\psi) G(\psi) dS \neq 0$ where $H(\psi)$ is some geometric factor. The procedure is then as follows:

First choose ψ^o and λ^o such that $I^o = \int \lambda^o H(\psi^o) G(\psi^o) dS \neq 0$ and has the same sign as I_p, a chosen value for this integral. We set $\lambda^1 = I_p \lambda^o / I^o$ and then solve $L\psi^1 = -\lambda^1 G(\psi^o)$. λ^1 is scaled and the process repeats until convergence is achieved. We have again used iterative methods to invert L.

When $G(\psi)$ is of a form which allows values of opposite signs the above iteration has been known to produce physically meaningless answers. Sykes /*4/ has extended the range of convergence by exploiting the non-linearity of (36). He uses a form of nonlinear SOR /*5/ in which each local equation is treated by the secant method. Thomas/*6/ has used nonlinear SOR in its full form. After several steps the eigen value λ is updated in the above manner. These 2 methods are now standard in our codes, so a capacitance matrix approach is no longer relevant, although it would have been if we had continued to use inverse iteration. Our experience with this type of problem helps to emphasise the fact that use of the simplest method can sometimes reduce the range of computable solutions.

In the third class of problem, the plasma is kept away from the shell by a device called a limiter, and the region between the plasma and the shell is vacuum. The location of the plasma boundary is a priori unknown and is part of the solution to the problem. Since the pressure is constant on a ψ surface we may pose our plasma vacuum equilibrium equation as

$$r\frac{\partial}{\partial r}\left(\frac{1}{r}\frac{\partial\psi}{\partial r}\right) + \frac{\partial^2\psi}{\partial z^2} = -FF' - r^2p' \quad \text{if} \quad \psi \geq \psi_p$$

$$= 0 \quad \text{if} \quad \psi \leq \psi_p \qquad (37)$$

with $\psi = \psi_W$ on the shell and $\psi_W < \psi_p$. Since $\psi_W < \psi_p$, $\psi = \psi_W$ is a trivial solution to (37) and hence we must again look for eigenvalues in order to obtain a physically interesting solution.

The treatment of (37) is similar to that of (36) but we now have a broader choice of parameters to consider as eigenvalues. If we write the r.h.s. of (36) as $-\lambda G(\psi)$, there are 3 common choices of eigenvalues (1) λ (2) ψ_p (3) λ and ψ_p. In case (1) ψ_p is fixed and λ is varied so that the integral I converges to its specified value. In case (2) λ is fixed and ψ_p is taken as the value of ψ at each iteration at some specified point. This specified point is chosen so that the plasma boundary lies within the limiter. In case (3) procedures (1) and (2) are applied simultaneously. Several simple rules have been derived for choosing the fixed point in order to guarantee convergence, see /*3/. Inverse iteration and nonlinear SOR have both been applied to this problem at Culham and once again the capacitance matrix approach has not been applicable. Examples of problems in these 3 classes are given by Thomas and Haas /137/.

The fourth class of equilibria is applicable to experiments which do not have a copper shell. We have no natural boundary and no simple boundary condition. Hence, provided we have some physical principle which tells us how to construct a boundary condition we have a free choice of boundary. To allow us to use a fast Poisson solver we have used a rectangular boundary. The boundary is placed so as to lie inside all the conductors and outside the expected plasma boundary. The boundary conditions are computed from the property that at any point the vector potential is the sum of the vector potentials due to the conductor currents and the vector potentials due to the plasma currents. Constraints are applied as in the above class of equilibria. The derivation of the difference equations is performed by the previously mentioned integral technique. It was found by Thomas /135/, that mesh cells which cross the plasma-vacuum interface have to be modified so that the integral of the r.h.s. is performed completely in the plasma. This was

necessary to maintain convergence as the mesh size is reduced to zero. The present version of the Culham code /136/ uses inverse iteration so we are able to incorporate the Bunemann algorithm provided the number of points in each direction is $2^m + 1$.

In straight geometry the local equation is

$$\frac{\psi_{i+1j} - 2\psi_{ij} + \psi_{i-1j}}{\Delta_x^2} + \frac{\psi_{ij+1} - 2\psi_{ij} + \psi_{ij-1}}{\Delta_y^2} = - \frac{A_{ij}\, j_{zij}}{\Delta_x^2 \Delta_y^2} \tag{38}$$

where A_{ij} is the area of the mesh cell taking account of the interface, wherever necessary. Hence ordering the points along the rows, the set of difference equations is

$$\begin{bmatrix} A & I & & & \\ I & A & I & & \\ & \ddots & \ddots & \ddots & \\ & & I & A & I \\ & & & I & A \end{bmatrix} \begin{bmatrix} x_2 \\ x_3 \\ \cdot \\ \cdot \\ x_{n-2} \\ x_{n-1} \end{bmatrix} = \begin{bmatrix} y_2 \\ y_3 \\ \cdot \\ \cdot \\ y_{n-2} \\ y_{n-1} \end{bmatrix} \tag{39}$$

where A is the tridiagonal matrix

$$\begin{bmatrix} -\lambda & 1 & & & \\ 1 & -\lambda & 1 & & \\ & \ddots & \ddots & \ddots & \\ & & 1 & -\lambda & 1 \\ & & & 1 & -\lambda \end{bmatrix}$$

$\lambda = 2\left(1 + \frac{\Delta_y^2}{\Delta_x^2}\right)$ and $\underline{x}_k^T = (\psi_{2k}, \psi_{3k}, \ldots, \psi_{n-1k})$, the kth row in the y direction and y_k^T are vectors of j_{zij} and include the boundary terms. We remark that the number of rows must be $n = 2^m + 1$ (including top and bottom) but the number of columns is unimportant since we invert A by the tridiagonal version of Gaussian elimination.

In axisymmetric geometry the local difference equation may be written as

$$\frac{\psi_{i+1j} - \psi_{ij}}{(r_i + \frac{1}{2}\Delta r)} \frac{\Delta z^2}{\Delta r^2} + \frac{\psi_{i-1j} - \psi_{ij}}{(r_i - \frac{1}{2}\Delta r)} \frac{\Delta z^2}{\Delta r^2} + \frac{\psi_{ij+1} - \psi_{ij}}{r_i} + \frac{\psi_{ij-1} - \psi_{ij}}{r_i} = - j_{\varphi_{ij}} \frac{\Delta z^2 A_{ij}}{\Delta r^2 \Delta z^2} \tag{40}$$

and the set of difference equations is

$$\begin{bmatrix} \hat{A} & D & & & \\ D & \hat{A} & D & & \\ & \ddots & \ddots & \ddots & \\ & & D & \hat{A} & D \\ & & & D & \hat{A} \end{bmatrix} \begin{bmatrix} \hat{x}_2 \\ \hat{x}_3 \\ \vdots \\ \hat{x}_{n-2} \\ \hat{x}_{n-1} \end{bmatrix} = \begin{bmatrix} \hat{y}_2 \\ \hat{y}_3 \\ \vdots \\ \hat{y}_{n-2} \\ \hat{y}_{n-1} \end{bmatrix}$$

where $\hat{A}$ is the matrix

$$\begin{bmatrix} b_2 & c_2 & & & \\ a_3 & b_3 & c_3 & & \\ & \ddots & \ddots & \ddots & \\ & & a_{n-2} & b_{n-2} & c_{n-2} \\ & & & a_{n-1} & b_{n-1} \end{bmatrix} \quad \text{with} \quad b_i = -\frac{2}{r_i} - \left(\frac{1}{r_i + \frac{1}{2}\Delta r} + \frac{1}{r_i - \frac{1}{2}\Delta r} \right) \frac{\Delta z^2}{\Delta r^2}$$

$$\text{and} \quad c_i = \frac{\Delta z^2}{(r_i + \frac{1}{2}\Delta r)\,\Delta r^2}$$

and $\hat{D}$ is the matrix

$$\begin{bmatrix} d_2 & & \\ & \ddots & \\ & & d_{n-1} \end{bmatrix} \quad \text{with} \quad d_i = \frac{1}{r_i}$$

This system of equations is easily transformed to the form (39) as required by the Bunemann algorithm by setting

$$A = D^{-\frac{1}{2}} \hat{A} D^{-\frac{1}{2}}$$

$$\underline{x}_i = D^{\frac{1}{2}} \hat{\underline{x}}_i$$

$$\underline{y}_i = D^{-\frac{1}{2}} \hat{\underline{y}}_i \ .$$

An example of this last class of equilibria is given in Section 6.

6. EXAMPLES

In this section we give 2 examples of the efficiency and accuracy of the methods described above.

Example 1 is the computation of the axisymmetric magnetic field in Fig.7. The field is produced by direct current in the conductors and enhanced by the iron core. The permeability of the iron is given a constant value ($\mu/\mu_o = 100$). This is only approximate since physically μ varies with $|\underline{H}|$. In the experimental situation the iron core is not

axisymmetric. Fig. 7 shows the configuration at $\theta = 0^{\circ}$ and $\theta = 180^{\circ}$ only. A 35 × 50 variable mesh was placed carefully across the iron-air interface and the conductor boundaries. SLOR was used with $\omega = 1.855$ and convergence to 4 figures was obtained in 200 iterations. The total time for the run was 3 mins 44 secs on an ICL 4/70, store cycle time 1.4 μsec. This is the time to read in and check the data, set up and solve the difference equations, compute the field components, plot the field lines and perform various line integrals along them. The acceptable accuracy of the solution, bearing in mind the above approximations, is demonstrated in Fig. 8.

Example 2 is a theoretical study of the equilibrium of a straight constant current density plasma in a quadrupole field as shown in Fig. 9. Strauss /*7/ has shown that for a fixed plasma height and external field data, the height to width ratio of the plasma is a particular function of the value of the current density. We have run our code /136/ on this problem and the results for a 33 × 33 grid and a 65 × 65 grid are shown in Fig. 10. The convergence as the mesh size → 0 is clear. For the 33 × 33 grid typical number of iterations are 11 and typical timings are 89 secs. For the 65 × 65 grid the numbers are 11 iterations and 432 secs respectively. The timings include up-dating the boundary values twice and plotting the field lines.

CONCLUSION

We have indicated how elliptic equations occur in fusion research. These examples are by no means all the elliptic equations in this field, but are typical of those equations which have been solved numerically at Culham Laboratory.

In the main the finite difference method and iterative methods of solution have proved adequate for the situations where fast Poisson solvers are not applicable. Field problems with sloping interfaces are solved with reasonable accuracy in the potential but the accuracy in the fields is somewhat worse. This is clearly an area where finite elements come into their own. Iterative methods have also proved adequate where non-linear problems are concerned. Nonlinear SOR has a wider range of convergence than Picard's method, but problems with non positive definite matrices are not solvable by either method.

ACKNOWLEDGEMENTS

I should like to acknowledge the work of Dr B. Allen, J. Phillpott and H Salwan who were responsible for an earlier version of POTENT. I should also like to thank Dr F.A. Haas, Professor K.W. Morton and Dr P.F. Little who have all helped with their advice while this work was being done.

REFERENCES

(see the collection of references at the end of this volume)

SUPPLEMENTARY REFERENCES

/*1/ LITTLE, P.F. Private Communication

/*2/ RICHTMYER, R.D. and MORTON, K.W. Difference Methods for Initial Value Problems (1969), Interscience Publishers, New York.

/*3/ FENEBERG, W., and LACKNER, K. Multipole Tokamak Equilibria, Nuclear Fusion, 13, 549 (1973).

/*4/ SYKES, A. Private Communication

/*5/ ORTEGA, J.M. and RHEINBOLDT, W.C. Iterative Solution of Nonlinear Equations in Several Variables, (1970), Academic Press, New York.

/*6/ THOMAS, C.Ll. Unpublished

/*7/ STRAUSS, H.R. Bifurcation of Elliptic Equilibrium. The Physics of Fluids, 17, 1040, (1974).

REFERENCES

133 C.Ll. Thomas, POTENT - a package for the numerical solution of potential problems in general two dimensional regions, in Software for Numerical Mathematics (Ed. D.J. Evans) Academic Press, London and New York, 1974.

134 C.Ll. Thomas, THREE D - a digital computer code for the design and analysis of three dimensional electrostatic fields, in Computer Aided Design, IEE Conference Publication No. 111, 1974.

135 C.Ll. Thomas, The Numerical Calculation of Axisymmetric MHD Equilibria in Discrete Conductor Configurations, in Computational Methods in Classical and Quantum Physics (Ed. M.B. Hooper) Transcripter Books, 1977.

136 C.Ll. Thomas, The Computation of Multipole MHD Equilibria in Axisymmetric and Straight Geometry, UKAEA Research Group Report CLM-R 166, 1977.

137 C.Ll. Thomas and F.A. Haas, Computation of MHD Equilibria in Tokamak, UKAEA Research Group Report CLM-R 133, 1974.

140 E.L. Wachspress, Iterative Solution of Elliptic Systems, Prentice Hall, 1966.

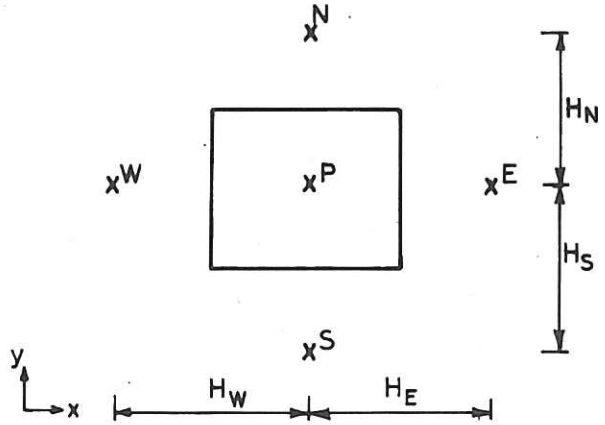

Fig.1 Mesh cell for difference equation in (x, y) coordinates.

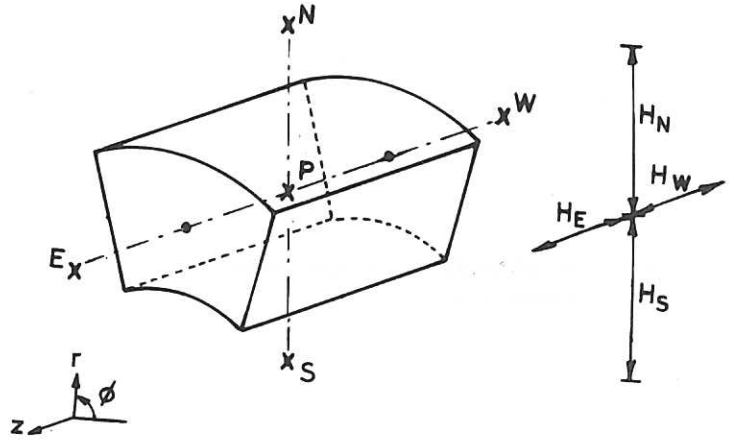

Fig.2 Mesh cell for difference equation in (r, z) coordinates ($r \neq 0$).

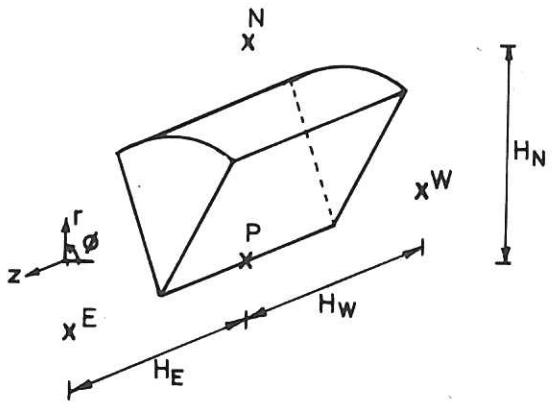

Fig.3 Mesh cell for difference equation in (r, z) coordinates ($r = 0$).

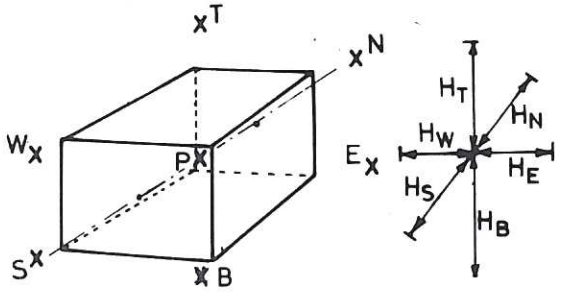

Fig.4 Mesh cell for difference equation in three dimensions.

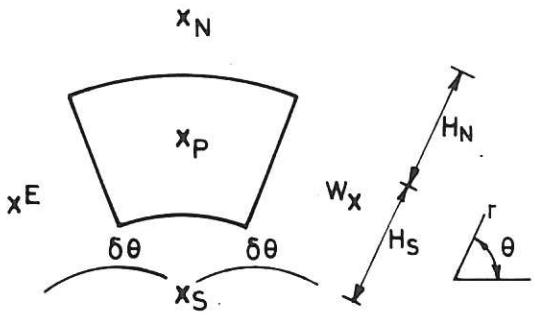

Fig.5 Mesh cell for difference equation in toroidal polar coordinates ($r \neq 0$).

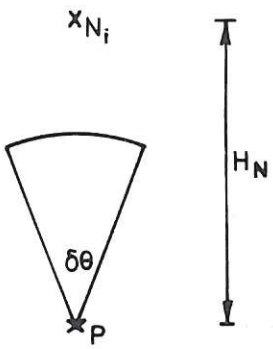

Fig.6 Mesh cell for difference equation in toroidal polar coordinates ($r = 0$).

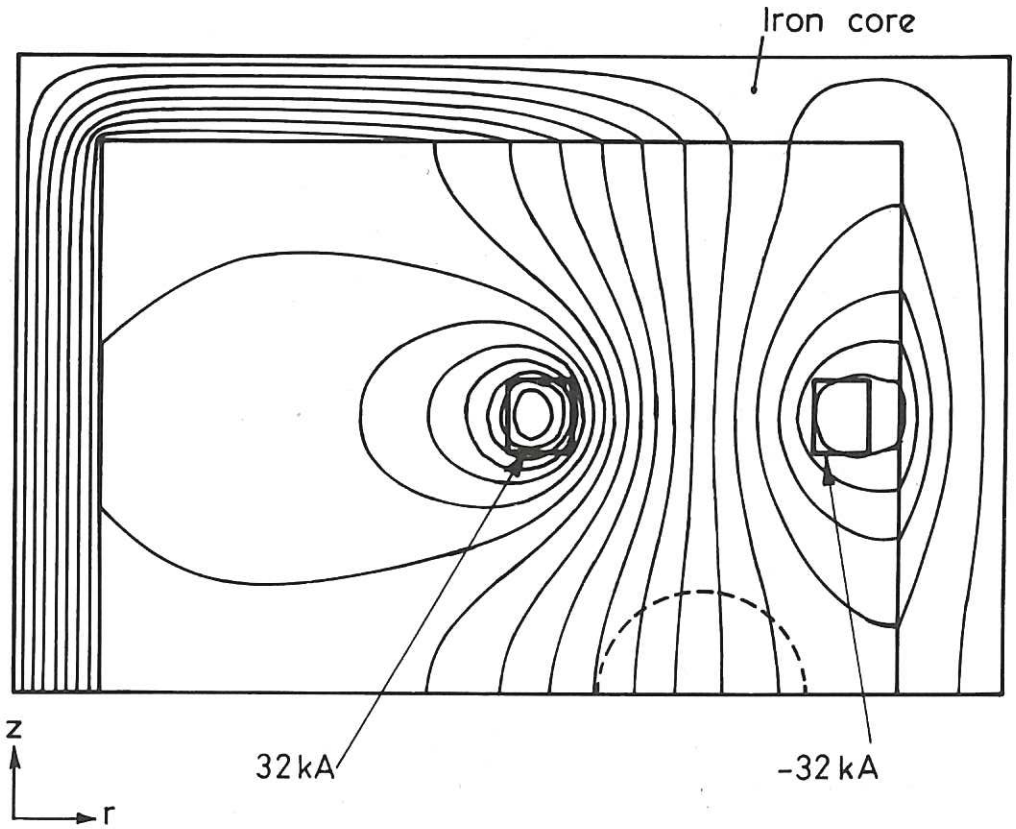

Fig.7 Example of a vacuum magnetic field produced by direct current and enhanced by an iron core. The dotted curve is the expected position the plasma would take up. Dimensions are 108 cms in the z direction and 162 cms in the r direction. The flux is given a constant value of zero along the outer iron boundary.

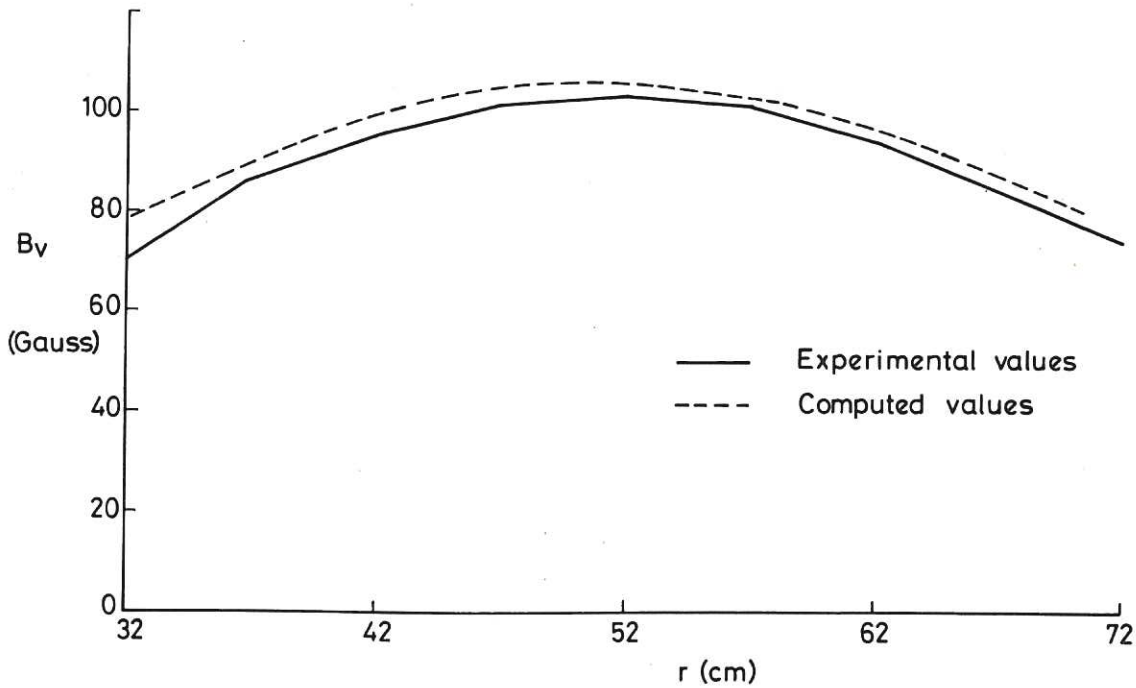

Fig.8 Comparison between computed and experimental values of the vertical field in the region of the plasma in Fig.7.

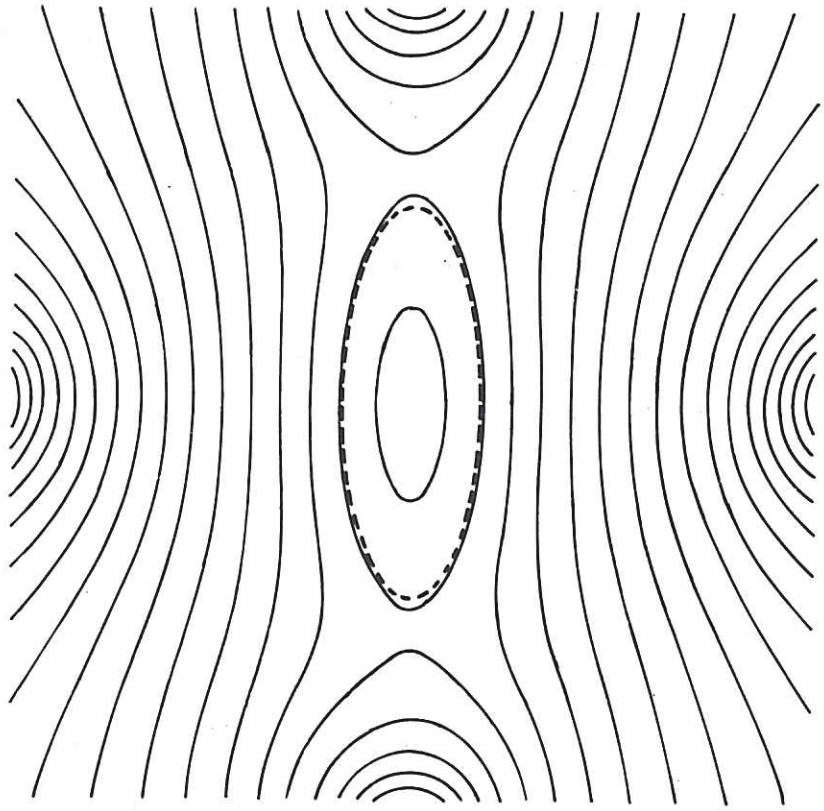

Fig.9 Solution of the equilibrium of a straight constant current density elliptic plasma in a quadrupole field. The plasma lies inside the broken line. The quadrupole conductors lie within the closed surfaces outside the plasma. The conductors above and below the plasma carry current in the same direction as the plasma current.

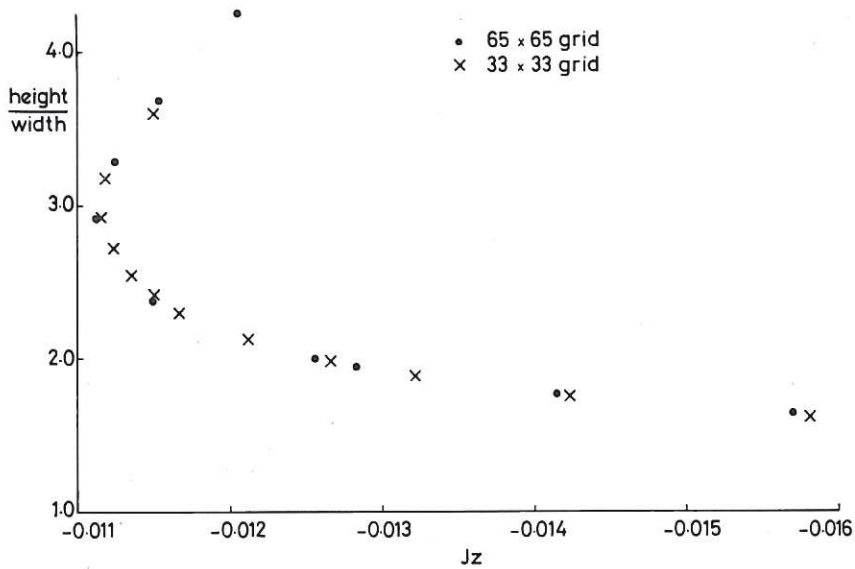

Fig.10 Plot of height to width ratio against current density of the plasma in Fig.9. This curve is obtained by keeping the external field data fixed and varying the total plasma current.